Iron oxide thin films grown on (00l) sapphire substrate by pulsed-laser deposition

C-E Bejjit, V. Rogé, C. Cachoncinlle, C. Hebert, J. Perrière, E. Briand, E. Millon

Iron oxide thin films grown on (00l) sapphire substrate by pulsed-laser deposition

C-E Bejjit[1], V. Rogé[1§], C. Cachoncinlle[1], C. Hebert[2,3], J. Perrière[2,3], E. Briand[2,3], E. Millon[1*]

[1] GREMI, UMR 7344 CNRS / Université d'Orléans, 14 Rue Issoudun, 45067 Orléans Cedex 2, France
[2] Sorbonne Universités, UPMC Paris 06, UMR 7588, INSP, 4 Place Jussieu, 75005 Paris, France
[3] CNRS, UMR 7588, INSP, 4 Place Jussieu,75005 Paris, France

* : Corresponding author : email : eric.millon@univ-orleans.fr
§ : Present address : LIST, 41 rue de Brill, L-4422 Belvaux, Luxembourg

Abstract :

Magnetite (Fe_3O_4) and wustite (FeO) are well-known oxides for their promising magnetic properties. However, growing stable FeO_x thin films with controlled iron oxidation states could be of interest for further applications. In this work, we highlight the formation of different FeO_x-based thin films grown by pulsed-laser deposition (PLD) from Fe or α-Fe_2O_3 targets onto sapphire substrates. Based on X-ray diffraction and Rutherford backscattering spectroscopy analyses, we report on films with various O/Fe ratios obtained by controlling both the substrate temperature and the oxygen pressure in the 10^{-5} – 10 Pa range during the PLD growth. Thus, the different crystalline phases of the Fe-O system can be grown: metallic iron, α-Fe_2O_3, Fe_3O_4, and the thermodynamically metastable phase FeO. On one hand, we demonstrate that at low pressures (< 10^{-4} Pa) metal-oxide composite thin films with both metallic Fe and Fe_3O_4 phase are epitaxially grown on the sapphire substrates even at room temperature. On the other hand, we highlight that using a α-Fe_2O_3 target, films composed with a mixture of wustite and spinel phases have been obtained at room temperature. The precise growth conditions leading to the formation of FeO-based films or metal-oxide composite films are discussed.

Keywords : pulsed-laser deposition, iron oxide, wustite, magnetite, epitaxy, nanocomposite,

Highlights :

* FeO-Fe_3O_4 composite 111-oriented films are grown at room temperature under 10^{-5} Pa
* metal-oxide composite films are epitaxially grown at room temperature from a Fe target
* Fe film grown at room temperature under vacuum shows a rectangle on hexagon epitaxy

Introduction

Iron oxide thin films have been studied for several decades for their potential applications due to their magnetic [1][2], catalytic [3], and sensing [4] properties. Regarding the Fe-O thermodynamical system, different phases ranging from α-Fe to $Fe_{1-x}O$ (wustite), Fe_3O_4 (magnetite), and α-Fe_2O_3 (hematite) can be obtained upon increasing the oxygen content and depending on the temperature. In particular, wustite and magnetite have been largely investigated due to their ferrimagnetic and unbalanced antiferromagnetic properties, respectively. For example, chemical vapor deposition [5] or rf-sputtering [2][6] methods may be classically used to obtain Fe_3O_4 thin films for ferrimagnetic properties [7]. By laser molecular beam epitaxy, Suturin et al. [8] have grown on (001) GaN substrate different magnetically ordered iron oxide phases, especially (111)-oriented Fe_3O_4 films were found to be epitaxied on the GaN substrate. If the growth of a single-phase Fe_3O_4 film is commonly observed, the main difficulty is the preferred stabilization of FeO instead of Fe_3O_4. By magnetization measurements, Kim et al. [2] have evidenced particular processing conditions during sputtering deposition that leads to a "ferrimagnetic $Fe_{1-x}O$" inside the spinel-based Fe_3O_4 film. Kozioł-Rachwa et al. [9] reported on the growth of monolayer-like FeO (001) films (0.17 nm thick) via molecular beam epitaxy on (001) MgO using the reactive deposition of Fe.

Fe_3O_4 films have also been obtained by pulsed-laser deposition (PLD) on (100) MgO substrate and these films exhibit a high structural order following a (100) Fe_3O_4 texturation and a perfect stoichiometry leading to the Verwey transition at 121 K [10]. Pure magnetite PLD films may be produced onto Si (100) [1], glass [11] or c-cut sapphire [12] substrates at relatively moderated growth temperatures (200-500°C) and under an intermediate range of oxygen pressure (10^{-3} to 10^{-2} Pa).

The thin film growth of wustite phase is more challenging due to the tendency of FeO first to decompose into spinel Fe_3O_4 and metal Fe below 575°C and, second to be easily oxidized to the higher valence oxides such as Fe_3O_4 and α-Fe_2O_3.

In this work, compositions, structures and morphologies of different oxide phases grown by PLD onto c-cut ((001) oriented) sapphire are studied. More specifically, the influence of substrates temperatures ranging from room temperature (RT) to 600°C and partial oxygen pressures ranging from 10^{-5} to 10 Pa are investigated. Our aim is to define the experimental growth conditions allowing the formation a single-phase film (oxide or metallic) Fe- on c-cut sapphire substrates. In this respect, a particular attention is paid to the stability domain (pressure, temperature) of wustite. In addition, we attempt to specify the experimental conditions leading to the formation mixed phases (i.e. metal/oxide composite). By means of two types of targets (Fe and α-Fe_2O_3), we evidence that the FeO phase can be grown at temperature below 575°C and that a nanocomposite film made of Fe and Fe_3O_4 can be produced with monitored experimental conditions.

Experimental

FeO_x films were deposited by PLD onto (001) c-cut sapphire single crystal substrates (Crystec Gmbh). Two types of targets were used to grow iron oxide films with different O/Fe ratios : a metallic polycrystalline Fe (99.99%) target and a hot pressed ceramic α-Fe_2O_3 (99.9%) one. They were ablated by a frequency quadrupled Nd:YAG laser (266 nm) with a 10 ns pulse duration under a repetition rate of 10 Hz in the experimental set-ups described previously [13][14]. The laser beam irradiates the target under an incidence angle of 45° with a laser energy kept constant at 25 mJ

leading to a laser fluence of around 2.5 J/cm^2. The distance between the target and the substrate was fixed at 5 cm. the oxygen pressure during films growth is varied from 10^{-5} Pa (the vacuum limit) to 10 Pa, in order to modulate the oxygen content in films [15]. Films obtained by laser ablation of the α-Fe_2O_3 target were grown under vacuum at different substrate temperatures (RT, 200, 300, 500, and 600°C) while the PLD of FeO_x films was obtained under the different oxygen pressures at RT and 500°C using the Fe target.

The determination of thickness and composition (O/Fe ratio) of films were obtained by Rutherford backscattering spectrometry (RBS) using the 2 MeV ion accelerator facilities of the Sorbonne Université (SAFIR). Due to the low RBS yield on light elements, the oxygen content of the films is determined with a 4% precision. The structural characterization of films was carried out by X-ray diffraction (XRD) experiments using an X-ray diffractometer (Bruker D8 Discover) with the CuKα radiation (λ=0.154 nm) in the Bragg Brentano condition for identifications of phases. In asymmetric geometry, pole figures and ϕ-scan measurements were performed to describe the texture and the epitaxial relationships between the films and the c-cut sapphire substrate [16]. Scanning electron microscopy (SEM; Field Gun Zeiss Supra 40) was used to obtain information on the surface morphology of films. The images were obtained by collecting the secondary electrons with an in-lens detector and a working distance of 3.5 to 4.5 mm under a voltage of 3.0 to 4.0 kV.

Results and Discussion

The experimental growth conditions, the structural properties and the composition of the two sets of iron oxide films are presented below according to the target used (α-Fe_2O_3 and Fe). Tables 1 and 2 summarize the results obtained for FeO_x films grown from α-Fe_2O_3 and Fe targets, respectively.

Table 1 : composition and structural properties of FeO_x films obtained by laser ablation of a α-Fe_2O_3 target under 10^{-5} Pa at different temperatures.

Target	Substrate temp. (°C)	RBS O/Fe	XRD Phases	XRD 2θ (°) Fe_3O_4 (111)	a-axis parameter Fe_3O_4 (nm)	XRD 2θ (°) FeO (111)	a-axis parameter FeO (nm)
Fe_2O_3	RT	1.33	Fe_3O_4, FeO	17.94	0.855	36.37	0.427
	200	1.23	Fe_3O_4, FeO	18.24	0.842	36.35	0.428
	350	1.18	Fe_3O_4, FeO	18.32	0.839	36.18	0.429
	500	1.15	Fe_3O_4, FeO	18.32	0.839	36.18	0.429
	600	1.15	Fe_3O_4, FeO	18.36	0.836	36.18	0.429

Table 2 : composition and structural properties of FeO_x films obtained by laser ablation of a Fe target
at RT and 500°C under 3 oxygen pressures (the hematite phase is not taken into account in this table)

Target	O_2 pressure (Pa)	RBS O/Fe	XRD Phases	XRD 2θ (°) Fe (110)	a-axis parameter α-Fe (nm)
Fe	10 @RT	1.69	Fe_3O_4	-	-
	10^{-1} @RT	1.38	Fe_3O_4, Fe	44.69	0.286
	10^{-4} @RT	0	Fe	44.53	0.287

	10 @500°C	1.56	α-Fe_2O_3 , Fe_3O_4	-	-
	10^{-1} @500°C	1.47	α-Fe_2O_3, Fe	44.63	0.286
	10^{-4} @500°C	0.02	Fe	44.69	0.286

a) α-Fe_2O_3 ceramic target

To optimize the formation of the FeO suboxide phase with an O-rich target, one must limit the incorporation of oxygen coming from the surrounding gas and impinging onto the substrate surface during the PLD growth. FeO_x thin films have therefore been grown at RT, 200, 350, 500 and 600°C in vacuum limit conditions (10^{-5} Pa). Since the wustite phase in bulk form is stable above 575°C, moderate substrate temperatures have been applied to check the possible formation of this phase even at lower temperatures. Whatever the growth temperatures, films are dense and smooth, as observed on Fig. 1A which shows a typical SEM top view image of the film grown at RT with only few droplets.

The thickness of this film is around 200 nm for a deposition time of 2h leading to an average deposition rate of $2.5x10^{-3}$ nm/pulse. Such film is very smooth, and according to the SEM cross-section image (Fig. 1b), a columnar growth can be observed.

RBS spectra of our films (not shown here) evidence a uniform in-depth distribution of O and Fe elements. The O/Fe ratios deduced from these spectra (Table 1) range from 1.33 at RT to 1.15 at 600°C. These ratios are slightly greater than unity. The O/Fe ratio of pure magnetite is 1.33. For wustite let us remind that from a thermodynamical point of view, this phase is never matched the stoichiometry since the O/Fe ratio is in the range of 1.06 - 1.20 for bulk material [17], depending on the temperature. The obtained values at high temperatures (above 350°C) indicate that the O-content is of same order than the one expected for a FeO film. At low temperatures (below 300°C) the O-contents are not in agreement with a pure wustite film, and the formation of magnetite is required to reach the obtained O/Fe ratios (>1.20). It is also worth noticing that the O/Fe ratio decreases as the substrate temperature increases : at RT, the O/Fe (1.33) would indicate that the film is only constituted by the Fe_3O_4 phase while at 600°C the O/Fe ratio (1.15) would be consistent with the single phase FeO. In addition, the XRD diagrams show that the crystallized part of films is constituted by a mixture of Fe_3O_4 and FeO; a higher content of crystallized Fe_3O_4 phase being qualitatively observed at 600°C. An explanation for the decrease of the O/Fe ratio with the increasing of the temperature could be hypothesized with the presence of amorphous or poorly crystallized oxide phases in the films, such as iron hydroxides. Moreover, as amorphous phases cannot be evidenced by XRD, , it should not be excluded that amorphous iron hydroxide matter could be present in films, particularly for those grown at RT. Indeed, at low temperature, water molecules from residual air moisture present in the chamber could be incorporated in the film. . Although the PLD chamber is pumped under high vacuum, this phenomenon can occur as it has already been suggested by Beena et al. for In_2O_3 PLD films grown under vacuum [18]. A highest growth temperature (600°C) makes difficult the formation of hydroxides since the residual moisture in the chamber is negligible. This preferred formation of iron hydroxides may explain the higher value of O/Fe observed for FeO_x films obtained at RT. In summary, the obtained compositions indicate that the iron oxide films would be made of a mixture of Fe-O phases.

The $\theta/2\theta$ XRD diagrams recorded on FeO_x films grown under vacuum are presented in Fig. 2a.

For any substrate temperature, the magnetite (ICCD file : 01-071-6336) and the wustite (ICCD file : 00-006-0615) phases are present. Both FeO and Fe_3O_4 crystallites in these composite films are textured along the [111] direction perpendicular to the (001) sapphire basal plane. The a-axis

parameters of the magnetite and the wustite deduced from the peak position of the (111) diffraction line, are given in the Table 1. For the Fe_3O_4 film grown at 600°C, the "a" parameter is similar to the value of bulk magnetite (0.837 nm). The same "a" parameter increases with the decrease of the temperature, indicating that tensile stresses occur during growths at low temperatures. On the contrary, the a-axis parameter of the wustite ranges from 0.427 nm at RT to 0.429 nm at 600°C. Those values are lower than the bulk one (0.431 nm). The narrowing of the "a" parameter indicates a compression of the FeO unit cell. It is important to note that FeO is formed even at RT and its crystallization is improved by the increase of the temperature, as attested by the decrease of the diffraction peak width.

The possible epitaxial relationships of the Fe_3O_4 and FeO crystallites on the c-cut substrate have been studied by pole figure measurements. Fig 2b (left part) shows the pole figures of the (200) wustite diffraction line recorded at $2\theta = 42.5°$ for the FeO_x film obtained at RT. Six well-defined poles are present at the tilting angle $\psi = 54.7°$, the expected value for the (111) texture of wustite crystallites. Similarly, the pole figure, recorded on the (220) Fe_3O_4 reflection at $2\theta = 29.8°$ also shows 6 poles with hexagonal symmetry at $\psi = 35.2°$, in agreement with the 111 Fe_3O_4 texture (Fig. 2b, right part). Finally, the following epitaxial relationships could be inferred from the two phases :

Magnetite : (111) Fe_3O_4 // (002) Al_2O_3 and [10-1] Fe_3O_4 // [210] Al_2O_3 (30° rotation) (I)

Wustite : (111) FeO // (002) Al_2O_3 and [10-1] FeO // [210] Al_2O_3 (30° rotation) (II)

These relationships imply a 30° rotation of the hexagons of the (111) FeO and (111) Fe_3O_4 planes with respect to the hexagonal (001) basal plane of the c-cut sapphire substrate.

Regarding the Fe_3O_4 crystallites, such in-plane epitaxial relationships (I) with a "30° rotation" have already been reported for $Zn_{1-x}Fe_xO$ films grown by PLD under vacuum at 500°C on c-cut sapphire [19][20]. These (111)-oriented Fe_3O_4 films are the result of a particular growth induced by the c-cut sapphire substrate used. Indeed, it has been observed that magnetite films grown by PLD under 10^{-3} Pa oxygen pressure at 350°C onto Si (100) substrate are polycrystalline, exhibiting a (311)-preferred orientation [1]. On the contrary, the use of fused quartz substrate leads to the predominant (110) texture for the magnetite thin films obtained by PLD after annealing at 10^{-4} Pa at 500°C [11]. The growth of 111- textured magnetite film on c-cut sapphire by PLD has already been observed recently by Malikov et al. [21] at moderate substrate temperature (300 - 500°C) under 10^{-3} Pa. Regarding the growth of FeO crystallites on c-cut sapphire substrate, the epitaxial relationships (II) evidenced here have not been reported elsewhere. The origin of the epitaxy of (111) FeO onto (002) Al_2O_3 can be found in the electrostatic interactions between these planes since (002) Al_2O_3 and (111) FeO are both polar (i.e. constituted either by cations or anions).

We show here that the growth of FeO-based films is obtained below 575°C by ablating a α-Fe_2O_3 target under high vacuum, but the wustite is always present with the Fe_3O_4 phase. Films constituted by a mixture of 2 phases FeO and Fe_3O_4 are classically grown for a substrate temperature greater than 600°C [22], and the growth of « pure » FeO film may be obtained by doping the target (for example by Si or In [23]) to stabilize the wustite phase. Below 600°C, the FeO_x films are generally mixed with the magnetite phase [1][24], but the presence of wustite in film grown below 600°C has not been yet reported. As determined by asymmetric diffraction, our films are also found to be epitaxied on the c-cut sapphire substrate even at RT.

b) Fe metallic target

The use of a non-oxide target, which avoids the incorporation of oxygen coming from the ablated material, allows to expect the formation of low valence state (i.e. Fe^{2+}) oxide in films. Indeed, the flux of oxygen species impinging onto the substrate during the growth is easily controlled by the oxygen pressure in the PLD chamber. That is the reason why a Fe metallic target was used. Oxygen incorporation in films results from interactions between the plasma plume and its surrounding gas. In order to modulate the O-content in films, 3 different oxygen pressures have therefore been applied during the growth : 10^{-4} , 10^{-1} and 10 Pa. In addition, the growth of films has been performed at substrate temperatures of 25°C (RT) and 500°C. The main drawback related to the use of a metallic target is the unsuitable formation of droplets due to the thermal effects, which is more important than for a ceramic (oxide) target. By reducing the laser fluence, it is possible to obtain Fe-based films with a very limited content of droplets. Fig 3 shows typical SEM top view of films depending on the growth conditions. Besides some visible droplets, films are relatively smooth, especially at RT under 10^{-4} Pa. By increasing both the pressure and the substrate temperature, a granular morphology is revealed, and some cracks appear on the surface.

At higher pressures (10^{1} Pa), elongated needle-shaped crystallites are formed. The formation of faceted crystallites and the increase of surface roughness of films with the pressure is a well-known feature, already described since a long time for PLD films [25][26].

RBS analysis has been performed on the obtained films. The O/Fe ratios deduced from the spectra (not shown here) are presented in the Table 2. At RT and 10^{-4} Pa, the oxygen in the film is not detected, meaning that the film is mostly constituted by metallic Fe. At higher temperature (500°C) and at the same pressure, the O/Fe ratio is found to be around 0.01, indicating a weak incorporation of oxygen in the film. At higher pressures (10^{-1}, 10 Pa), the O/Fe ratio is ranging from 1.3 to 1.7, in agreement with the formation of an oxide-based film, and it can be noticed that these ratios are higher than expected for a pure FeO film. From the RBS spectra, it is also possible to get a rough estimation of the number of Fe atoms/cm^2 impinging onto the substrate during the growth at each laser pulse, considering that all Fe atoms coming from the plasma plume are sticked on the substrate without any losses. In the case of films grown at 500°C, the obtained values of the number of iron atoms N_{Fe} are $2.4x10^{13}$, $1.1x10^{13}$, and $0.5x10^{13}$ at cm^{-2} $pulse^{-1}$ for the three oxygen pressures 10^{-4}, 10^{-1} and 10 Pa, respectively. The oxygen incorporated in the film is only coming from the background gas since a metallic target is used. By considering the kinetic theory of gas and assuming that O_2 would be an ideal gas, a rough estimation of the number density N_{O2} of oxygen molecules arriving on the substrate is :

$$N_{O2} = N_a (P\Delta t/RT)(3RT/M_{O2})^{1/2}$$

with $N_a=6.02x10^{23}$ at mol^{-1}, R=8.31 J K^{-1} mol^{-1}, M_{O2}=32 g mol^{-1}, T=773K, and Δt=1 µs. Δt is the approximate time during which the ablated species are transferred from the target to the substrate for a typical target to substrate distance of 5 cm [27]. This relationship leads to N_{O2} values of $7.3x10^{12}$, $7.3x10^{15}$, and $7.3x10^{17}$ molecule $cm^{-2}pulse^{-1}$ at pressures P of 10^{-4}, 10^{-1} and 10 Pa, respectively. By comparing N_{Fe} with N_{O2}, one figures that oxygen pressures above 10^{-1} Pa induce a higher oxygen flux than that of the iron one which leads to formation of oxide phases in the films, as observed experimentally.

The $\theta/2\theta$ XRD diagrams confirm the incorporation of oxygen at elevated pressures and allow to determine the nature of phases. On XRD patterns depicted in Fig 4, different phases can be identified : metal iron α-Fe cubic phase (ICCD file : 00-006-0615), magnetite (ICCD file : 01-071-6336) and hematite α-Fe_2O_3 (ICCD file : 00-033-0664), depending on the temperature and the oxygen pressure. At RT, under vacuum, a pure Fe film is obtained. However, with an increasing of the pressure, i.e. at 10 Pa, the film is oxidized in magnetite. For the higher temperature (500°C) and

above 10^{-1} Pa, films are composed of the α-Fe, Fe_3O_4 and α-Fe_2O_3 phases leading to a metal-oxide composite. At 10 Pa, metal Fe does not exist anymore, and the film is only constituted by a mixture of the magnetite and hematite α-Fe_2O_3 phases. At low pressure (10^{-4} Pa), only metal iron is observed, in agreement with RBS analyses. The growth by PLD of pure α-Fe films with a 110-texturation on c-cut sapphire has already been documented in the literature: by laser ablation of a Fe target, De La Cruz et al. [28] observed such texturation by growing films at RT under vacuum. Nevertheless, according to their experiments, for substrate temperatures above 450°C, the 200-texturation takes place. This is not in agreement with our results for which the 200-orientation of α-Fe crystallites is not evidenced. Finally, it is important to note that the wustite phase is not present whatever the experimental conditions used, while a metal-oxide composite may be obtained under around 10^{-1} Pa.

Regarding the intensity of the peaks and their full width at half maximum (FWHM), the α-Fe phase is more crystalline than the oxide ones. A strong 110-texturation of the Fe crystallites is observed for films grown under 10^{-4} and 10^{-1} Pa regardless of the temperature. Specifically, a "pure" Fe film is obtained under vacuum and present a 110 texturation of iron crystallites. To check the angular distribution of the Fe crystallites along the [110] direction, ω-scans have been recorded on the 110 Fe reflection for films grown under vacuum at RT and 500°C, for a fixed 2θ position at 44.53° and 44.69°, respectively. The corresponding rocking curves are given on Fig. 5 : the FWHM of the peaks are 0.94° and 0.37°,respectively. These low values indicate a good mosaicity of films, the structural disorder being more important at low growth temperature (RT) as it is classically observed in PLD films.

On the contrary, different orientations can be noticed for the magnetite, and at RT under 10^{-1} Pa it is possible to grow a composite film constituted by both 110-textured α–Fe and 111-oriented Fe_3O_4. Pole figure measurements were realized on these two phases : the same angular positions (2θ = 29.8°, ψ = 35.2°) lead to a pole figure for the 220 Fe_3O_4 diffraction line exhibiting the 6-fold symmetry already observed for films obtained by laser ablation of α-Fe_2O_3 target (see paragraph “a”). To check the possible in-plane relationships of the 110-textured Fe film, a pole figure was performed on the “pure” Fe film grown at 500°C under vacuum (Fig. 6a).

The pole figure depicted on Fig 6a) shows 6 well-defined poles at declination angle ψ = 45°. The 6 observed poles could agree with a hexagonal symmetry, but in fact, due to the rectangular geometry of the (110) Fe plane involving a 2-fold symmetry, they correspond to 3 sets of 2 poles induced by the 3-fold symmetry of the rhombohedral Al_2O_3 basal plane. It may be found that the relationships reads:

Out-of-plane : (110) Fe // (002) Al_2O_3

In-plane : [-110] Fe // [210] Al_2O_3 and [001] Fe // [010] Al_2O_3

This relationships between the Fe film and the (001) Al_2O_3 does not correspond to a “hexagon on hexagon” epitaxy as it has been observed for FeO and Fe_3O_4 grown on c-cut sapphire. This is also not the classical “cube on cube” epitaxy observed for Fe film grown on (100) MgO substrate which are defined as : (100) Fe // (100) MgO and [011] FeO // [110] MgO [29]. Despite that 110-oriented Fe films grown on c-cut substrate have already been identified [28], the in-plane epitaxial relationship of such films has never been reported previously.

With this result, we may suggest a schematic view of the interface Film/Substrate based on the crystallographic directions involved in the epitaxy of (110) Fe film on (001) Al_2O_3 substrate (Fig. 6b). The observed “rectangle on hexagon” epitaxy is based on a good film/substrate mismatch

which can be described by the domain matching epitaxy (DME) approach [30]. The DME is based on the coincidence between “m” and “p” lattice units of the substrate and the film, respectively. The “m” and “p” values satisfy the following relation : $m_x d_s = p_x d_f$ with d_s and d_f being the respective distance between atoms (ions) in the substrate and the film on parallel directions. Thus :

- For [-110] Fe // [210] Al_2O_3, it is found m=1 and p=2 leading to a lattice mismatch of 1.70% and to an epitaxial domain size of 0.8 nm

- For [001] Fe // [010] Al_2O_3, it is found m=3 and p=5 leading to a lattice mismatch of 0.14% and to an epitaxial domain size of 1.4 nm

It is important to note that the use of a Fe target does not allow to obtain the wustite phase whatever the oxygen pressure, at RT or 500°C. The formation of FeO-based film under vacuum is effective by using a α-Fe_2O_3 target. On the contrary, the laser ablation of a Fe target only leads to the growth of an iron film or a metal-oxide Fe/Fe_3O_4 film depending on the oxygen pressure. This difference would indicate that the formation and the stabilization of FeO find its origin in the path related to the oxygen species arriving onto the substrate surface. The following hypotheses could be suggested:

- Using Fe target : oxygen species allowing the oxidation are O_2 molecules coming from the gas. The formation of FeO_x film is mainly due to the thermal oxidation of Fe on the substrate which is not in favor of FeO formation.

- Using α-Fe_2O_3 target : a great part of the oxygen incorporated in the film is due to various species (oxygen atoms, ions, excited) coming from the target and present in the plasma during the plume expansion. The high reactivity of these O species would enhance the formation of the metastable wustite phase.

Conclusions

The different phases α-Fe, $Fe_{1-x}O$, Fe_3O_4 , and α-Fe_2O_3 of the Fe-O system have been obtained by PLD on c-cut sapphire. The presence of these phases depends on the substrate temperature and the oxygen pressure, as it has largely been reported in the literature. Nevertheless, the nature of the target used for the ablation also plays a crucial role on the relative stability of the Fe-O phases, in addition to the substrate temperature and the oxygen partial pressure. Two major results are reported :

- A wustite-based film is only observed by using a α-Fe_2O_3 target at moderated substrate temperature (below 600°C) under high vacuum (below 10^{-4} Pa). Irrespectively from the substrate temperature (RT to 600°C), thin films constituted by a mixture of the wustite and Fe_3O_4 are formed. Below the temperature of thermodynamical stability of wustite (575°C), the wustite phase is always observed, even at RT. However, it cannot be grown without magnetite. These oxide composite films show noticeable crystallographic features : both FeO and Fe_3O_4 phases are 111-textured and show very well-defined epitaxial relationships with the (002) Al_2O_3 basal plane.

- A metal/oxide composite film constituted by a mixture of α–Fe and Fe_3O_4 can be formed at RT or 500°C, under intermediate pressure range (roughly around 10^{-1} Pa), when using a Fe target. The magnetite and the iron crystallites are (111) and (110) oriented, respectively. Both phases show in-plane epitaxial relationships with c-cut sapphire. Under 10^{-4} Pa, a pure α-Fe 110-oriented film is obtained at RT or 500°C. The in-plane epitaxial relationships between the α-Fe (110) crystallites and the c-cut sapphire substrate have been studied in detail and are found to be : [-110]Fe // [210]Al_2O_3 and [001]Fe // [010]Al_2O_3

Such epitaxy which has not been reported previously, can be correctly described by the domain matching epitaxy approach. Works are now in progress to investigate by HRTEM and STEM techniques the microstructural properties of composite films (the iron metal-wustite and the magnetite-wustite films) to highlight the orientations of crystallites inside the nanocomposite film.

Acknowledgements

The authors wish to thank Nicolas Dumuis and Nadjib Semmar for their assistance in PLD experiments. Charaf Bejjit acknowledges the french Region Centre Val de Loire for the financial support of his PhD position. The help of Amael Caillard and Sylvain Iseni has been highly appreciated concerning the fruitful discussions around the growth of thin films and the improvement of overall English language, respectively.

References

[1] M.L. Paramês, J. Mariano, M.S. Rogalski, N. Popovici, O. Conde, UV pulsed laser deposition of magnetite thin films, Materials Science and Engineering: B. 118 (2005) 246–249. https://doi.org/10.1016/j.mseb.2004.12.037.

[2] Y.K. Kim, M. Oliveria, Magnetic properties of reactively sputtered $Fe_{1-x}O$ and Fe_3O_4 thin films, Journal of Applied Physics. 75 (1994) 431–437. https://doi.org/10.1063/1.355869.

[3] R. Edla, A. Tonezzer, M. Orlandi, N. Patel, R. Fernandes, N. Bazzanella, K. Date, D.C. Kothari, A. Miotello, 3D hierarchical nanostructures of iron oxides coatings prepared by pulsed laser deposition for photocatalytic water purification, Applied Catalysis B: Environmental. 219 (2017) 401–411. https://doi.org/10.1016/j.apcatb.2017.07.063.

[4] S. Wang, W. Wang, W. Wang, Z. Jiao, J. Liu, Y. Qian, Characterization and gas-sensing properties of nanocrystalline ironžIII/ oxide films prepared by ultrasonic spray pyrolysis on silicon, (2000) 6.

[5] V. Sivakov, C. Petersen, C. Daniel, H. Shen, F. Mücklich, S. Mathur, Laser induced local and periodic phase transformations in iron oxide thin films obtained by chemical vapour deposition, Applied Surface Science. 247 (2005) 513–517. https://doi.org/10.1016/j.apsusc.2005.01.088.

[6] B. Mauvernay, L. Presmanes, S. Capdeville, V.G. de Resende, E. De Grave, C. Bonningue, Ph. Tailhades, Elaboration and characterization of Fe1–xO thin films sputter deposited from magnetite target, Thin Solid Films. 515 (2007) 6532–6536. https://doi.org/10.1016/j.tsf.2006.11.131.

[7] Y. Peng, C. Park, D.E. Laughlin, Fe3O4 thin films sputter deposited from iron oxide targets, Journal of Applied Physics. 93 (2003) 7957–7959. https://doi.org/10.1063/1.1556252.

[8] S.M. Suturin, A.M. Korovin, S.V. Gastev, M.P. Volkov, A.A. Sitnikova, D.A. Kirilenko, M. Tabuchi, N.S. Sokolov, Tunable polymorphism of epitaxial iron oxides in the four-in-one ferroic-on-GaN system with magnetically ordered α-, γ-, ε − Fe_2O_3 , and Fe_3O_4 layers, Phys. Rev. Materials. 2 (2018) 073403. https://doi.org/10.1103/PhysRevMaterials.2.073403.

[9] A. Kozioł-Rachwał, T. Ślęzak, T. Nozaki, S. Yuasa, J. Korecki, Growth and magnetic properties of ultrathin epitaxial FeO films and Fe/FeO bilayers on MgO(001), Appl. Phys. Lett. 108 (2016) 041606. https://doi.org/10.1063/1.4940890.

[10] D.M. Phase, S. Tiwari, R. Prakash, A. Dubey, V.G. Sathe, R.J. Choudhary, Raman study across Verwey transition of epitaxial Fe3O4 thin films on MgO (100) substrate grown by pulsed laser deposition, Journal of Applied Physics. 100 (2006) 123703. https://doi.org/10.1063/1.2403849.
[11] M. Bohra, N. Venkataramani, S. Prasad, N. Kumar, D.S. Misra, S.C. Sahoo, R. Krishnan, Study of pulsed laser deposited magnetite thin film, Journal of Magnetism and Magnetic Materials. 310 (2007) 2242–2244. https://doi.org/10.1016/j.jmmm.2006.10.822.
[12] S. Joshi, R. Nawathey, V.N. Koinkar, V.P. Godbole, S.M. Chaudhari, S.B. Ogale, S.K. Date, Pulsed laser deposition of iron oxide and ferrite films, Journal of Applied Physics. 64 (1988) 5647–5649. https://doi.org/10.1063/1.342258.
[13] M. Morcrette, A. Gutierrez-Llorente, W. Seiler, J. Perrière, A. Laurent, P. Barboux, Epitaxial growth of Pt and oxide multilayers on MgO by laser ablation, Journal of Applied Physics. 88 (2000) 5100–5106. https://doi.org/10.1063/1.1287781.
[14] E. Le Boulbar, E. Millon, J. Mathias, C. Boulmer-Leborgne, M. Nistor, F. Gherendi, N. Sbaï, J.B. Quoirin, Pure and Nb-doped TiO1.5 films grown by pulsed-laser deposition for transparent p–n homojunctions, Applied Surface Science. 257 (2011) 5380–5383. https://doi.org/10.1016/j.apsusc.2010.10.149.
[15] N. Chaoui, E. Millon, J.F. Muller, P. Ecker, W. Bieck, H.N. Migeon, Perovskite lead titanate PLD thin ®lms: study of oxygen incorporation by 18O tracing technique, Materials Chemistry and Physics. (1999) 6.
[16] N. Sbaï, J. Perrière, W. Seiler, E. Millon, Epitaxial growth of titanium oxide thin films on c-cut and α-cut sapphire substrates, Surface Science. 601 (2007) 5649–5658. https://doi.org/10.1016/j.susc.2007.09.019.
[17] H.A. Wriedt, The Fe-O (Iron-Oxygen) System, Journal of Phase Equilibria. 12 (1991) 170–200. https://doi.org/10.1007/BF02645713.
[18] D. Beena, K.J. Lethy, R. Vinodkumar, V.P. Mahadevan Pillai, V. Ganesan, D.M. Phase, S.K. Sudheer, Effect of substrate temperature on structural, optical and electrical properties of pulsed laser ablated nanostructured indium oxide films, Applied Surface Science. 255 (2009) 8334–8342. https://doi.org/10.1016/j.apsusc.2009.05.057.
[19] J. Perrière, C. Hebert, M. Nistor, E. Millon, J.J. Ganem, N. Jedrecy, $Zn_{1-x}Fe_xO$ films: from transparent Fe-diluted ZnO wurtzite to magnetic Zn-diluted Fe_3O_4 spinel, J. Mater. Chem. C. 3 (2015) 11239–11249. https://doi.org/10.1039/C5TC02090E.
[20] X. Portier, C. Hebert, E. Briand, J. Perrière, E. Millon, C. Cachoncinlle, M. Nistor, N. Jedrecy, Microstructure of nanocomposite wurtzite-spinel (Fe:ZnO)-(Zn:Fe3O4) epitaxial films, Materials Chemistry and Physics. 229 (2019) 130–138. https://doi.org/10.1016/j.matchemphys.2019.02.089.
[21] I.V. Malikov, V.A. Berezin, L.A. Fomin, G.M. Mikhailov, Epitaxial Growth of Fe3O4 Layers on the C-Plane of Sapphire by Pulsed Laser Deposition, Inorg Mater. 55 (2019) 42–48. https://doi.org/10.1134/S0020168519010072.
[22] Q. Guo, W. Shi, F. Liu, M. Arita, Y. Ikoma, K. Saito, T. Tanaka, M. Nishio, Effects of oxygen gas pressure on properties of iron oxide films grown by pulsed laser deposition, Journal of Alloys and Compounds. 552 (2013) 1–5. https://doi.org/10.1016/j.jallcom.2012.10.088.
[23] M. Seki, M. Takahashi, M. Adachi, H. Yamahara, H. Tabata, Fabrication and characterization of wüstite-based epitaxial thin films: p-type wide-gap oxide semiconductors composed of abundant elements, Appl. Phys. Lett. 105 (2014) 112105. https://doi.org/10.1063/1.4896316.
[24] S.G. Bhat, P.S. Anil Kumar, Investigation on the origin of exchange bias in epitaxial, oriented and polycrystalline Fe_3O_4 thin films, AIP Advances. 5 (2015) 117123. https://doi.org/10.1063/1.4935787.
[25] S. Choopun, R.D. Vispute, W. Noch, A. Balsamo, R.P. Sharma, T. Venkatesan, A. Iliadis, D.C.

Look, Oxygen pressure-tuned epitaxy and optoelectronic properties of laser-deposited ZnO films on sapphire, Appl. Phys. Lett. 75 (1999) 3947–3949. https://doi.org/10.1063/1.125503.
[26] W. Zhaoyang, H. Lizhong, Effect of oxygen pressure on the structural and optical properties of ZnO thin films on Si (111) by PLD, Vacuum. 83 (2009) 906–909. https://doi.org/10.1016/j.vacuum.2008.08.008.
[27] D.B. Chrisey, G.K. Hubler, eds., Pulsed laser deposition of thin films, J. Wiley, New York, 1994.
[28] W. De la Cruz, L. Cota Araiza, Epitaxial Growth and Characterization of Fe Thin Films on Sapphire by Laser Ablation, Physica Status Solidi (b). 220 (2000) 461–466. https://doi.org/10.1002/1521-3951(200007)220:1<461::AID-PSSB461>3.0.CO;2-X.
[29] J.F. Lawler, R. Schad, S. Jordan, H. van Kempen, Structure of epitaxial Fe films on MgO(100), Journal of Magnetism and Magnetic Materials. 165 (1997) 224–226. https://doi.org/10.1016/S0304-8853(96)00515-X.
[30] J. Narayan, Recent progress in thin film epitaxy across the misfit scale (2011 Acta Gold Medal Paper), Acta Materialia. 61 (2013) 2703–2724. https://doi.org/10.1016/j.actamat.2012.09.070.

Figure captions

Fig 1 : SEM top view (a) and cross section (b) of the FeO_x film grown at RT under 10^{-5} Pa from laser ablation of a α-Fe_2O_3 target

Fig. 2 : FeO_x films grown under vacuum by laser ablation of a αFe_2O_3 target.
a) $\theta/2\theta$ XRD patterns of films grown at different temperatures (the (006) Al_2O_3 peak located at 2θ= 41.68° corresponding to the c-cut sapphire substrate was removed).
b) Pole figures of the film grown at RT, recorded on the (200) FeO and (220) Fe_3O_4 diffraction lines at 2θ = 42.5° and 29.8°, respectively.

Fig 3 : SEM top view of the FeO_x films grown at RT (left) and 500°C (right) under 10, 10^{-1} and 10^{-4} Pa oxygen pressures by laser ablation of a Fe target

Fig. 4 : $\theta/2\theta$ XRD patterns of FeO_x films grown at RT (left) and 500°C (right) under different oxygen pressures by laser ablation of a Fe target

Fig. 5 : ω-scan recorded on the (110) Fe reflection of films grown at RT (left) and 500°C (right) under vacuum (10^{-4} Pa) by laser ablation of a Fe target. The 2θ angular position was fixed at 44.52° and 44.65°, respectively.

Fig. 6 : a) Pole figure recorded on the (200) Fe reflection at 2θ = 65° for a Fe film grown at 500°C under 10^{-4} Pa by laser ablation of a Fe target
b) Schematic view of the interface showing the matching between (110) Fe and (002) Al_2O_3 planes

Fig. 1

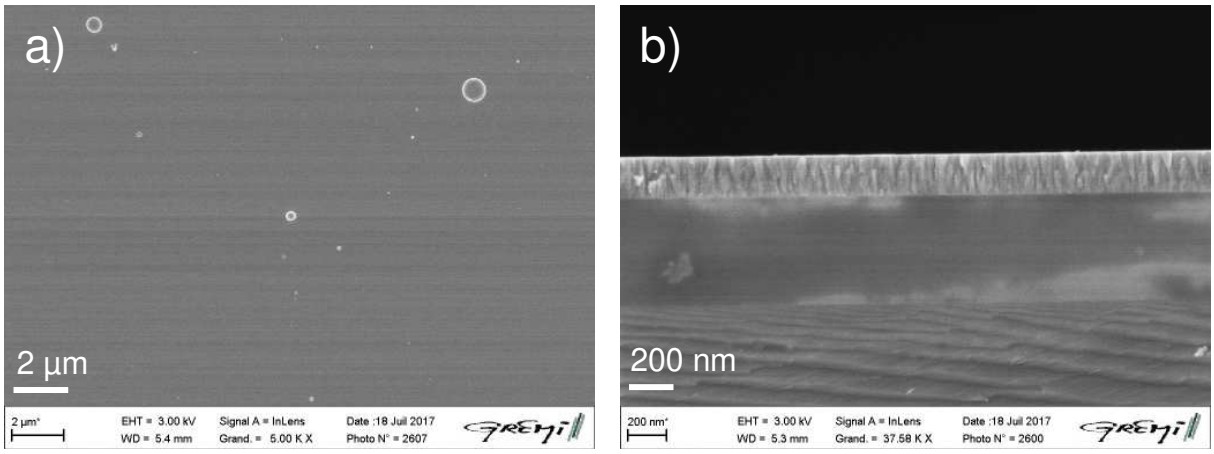
a)
2 µm
EHT = 3.00 kV
WD = 5.4 mm
Signal A = InLens
Grand. = 5.00 K X
Date :18 Juil 2017
Photo N° = 2607
b)
200 nm
EHT = 3.00 kV
WD = 5.3 mm
Signal A = InLens
Grand. = 37.58 K X
Date :18 Juil 2017
Photo N° = 2600

Fig. 2

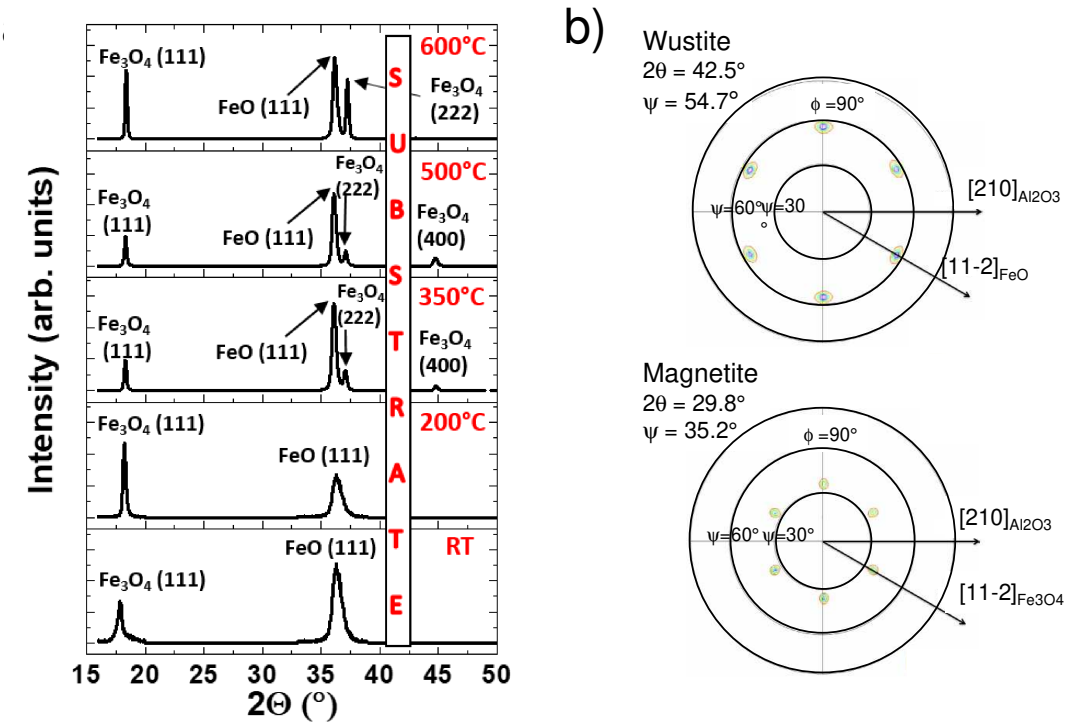
Intensity (arb. units)
2Θ (°)
15 20 25 30 35 40 45 50
600°C
500°C
350°C
200°C
RT
SUBSTRATE
Fe3O4 (111)
FeO (111)
Fe3O4 (222)
Fe3O4 (400)
b)
Wustite
2θ = 42.5°
ψ = 54.7°
ϕ =90°
ψ=60°
ψ=30°
[210]Al2O3
[11-2]FeO
Magnetite
2θ = 29.8°
ψ = 35.2°
ϕ =90°
ψ=60°
ψ=30°
[210]Al2O3
[11-2]Fe3O4

Fig. 3

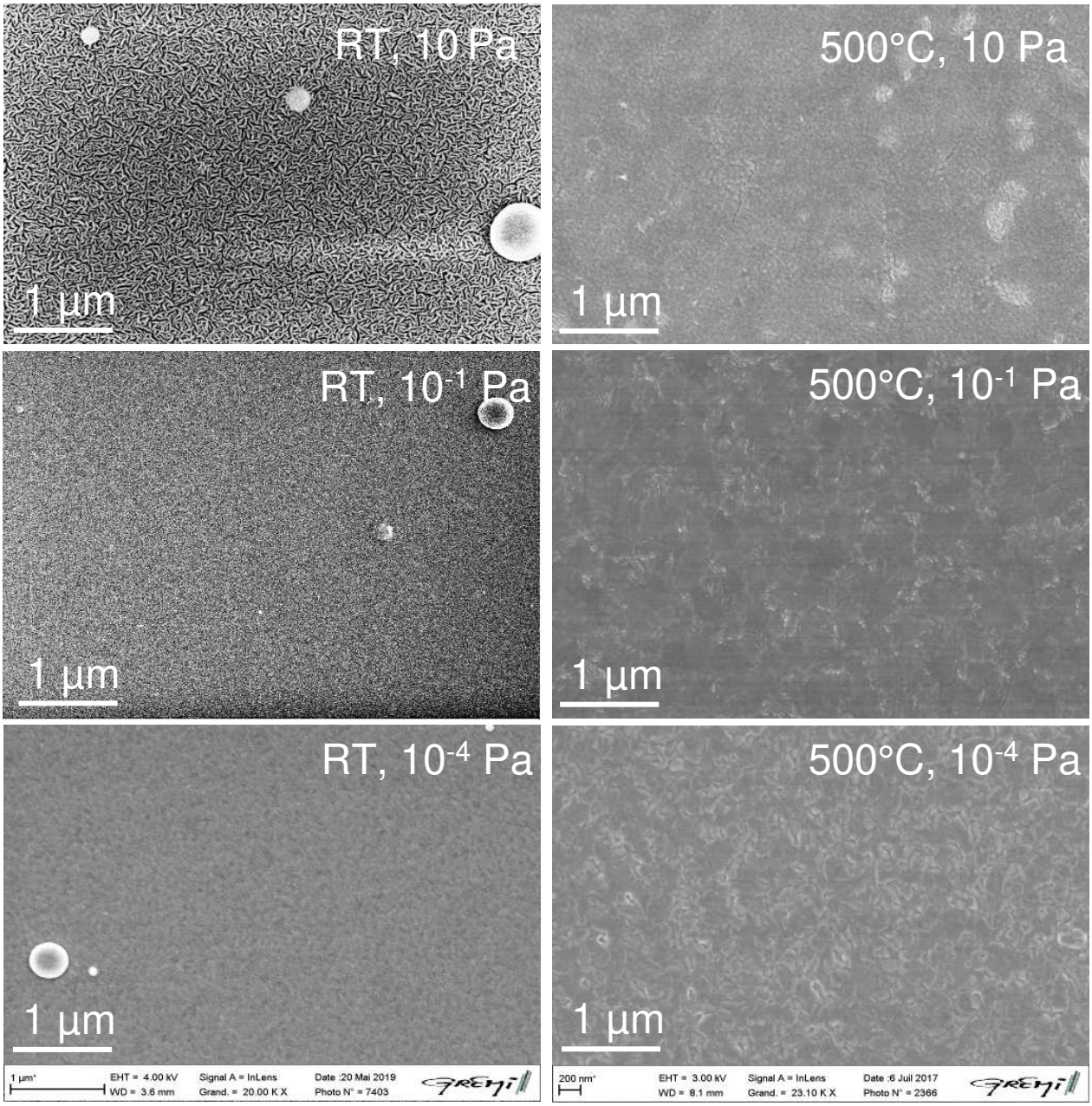
RT, 10 Pa
1 µm
500°C, 10 Pa
1 µm
RT, 10-1 Pa
1 µm
500°C, 10-1 Pa
1 µm
RT, 10-4 Pa
1 µm
1 µm* EHT = 4.00 kV WD = 3.6 mm Signal A = InLens Grand. = 20.00 K X Date :20 Mai 2019 Photo N° = 7403
500°C, 10-4 Pa
1 µm
200 nm* EHT = 3.00 kV WD = 8.1 mm Signal A = InLens Grand. = 23.10 K X Date :6 Juil 2017 Photo N° = 2366

FIg.4

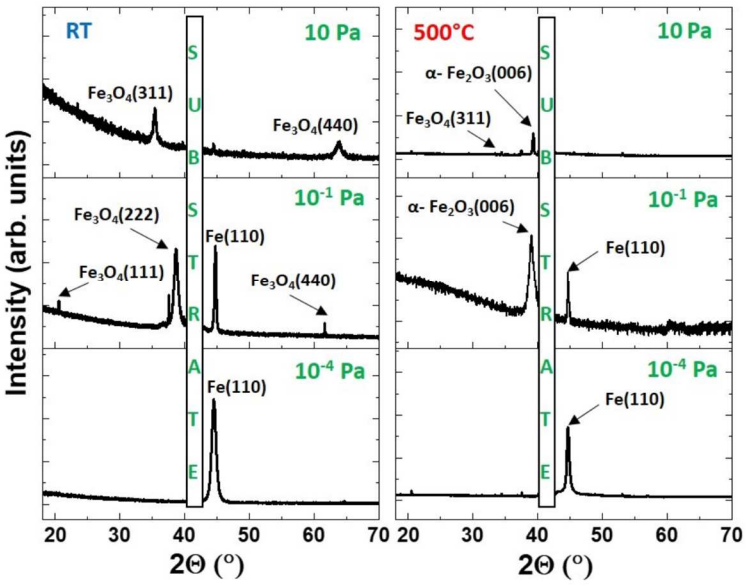

Fig.5

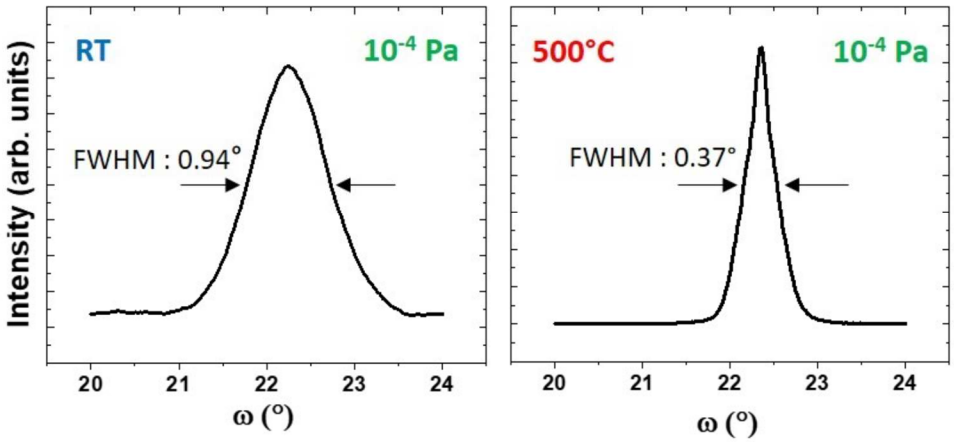

Fig .6